Since January 2020 Elsevier has created a COVID-19 resource centre with free information in English and Mandarin on the novel coronavirus COVID-19. The COVID-19 resource centre is hosted on Elsevier Connect, the company's public news and information website.

Antiviral Research 183 (2020) 104933

Contents lists available at ScienceDirect

Antiviral Research

journal homepage: www.elsevier.com/locate/antiviral

Research paper

A synthetic STING agonist inhibits the replication of human parainfluenza virus 3 and rhinovirus 16 through distinct mechanisms

Qingyuan Zhu *, Hui Hu, Haixia Liu, Hong Shen, Zhipeng Yan **, Lu Gao ***

Roche Innovation Center Shanghai, Shanghai, 201203, China

ARTICLE INFO

Keywords:
STING agonist
Parainfluenza virus
Rhinovirus
Autophagy
diABZI

ABSTRACT

Stimulator of interferon genes (STING), as a signaling hub in innate immunity, plays a central role for the effective initiation of host defense mechanisms against microbial infections. Upon binding of its ligand cyclic dinucleotides (CDNs) produced by the cyclic GMP-AMP synthase (cGAS) or invading bacteria, STING is activated, leading to the induction of both type I interferon responses and autophagy, which are critical for the control of certain microbial infections. RNA viruses, such as Parainfluenza virus (PIV) and Rhinovirus (HRV), are among the leading causes of respiratory infections that affect human health without effective treatments. Activation of STING pathway may provide a new therapeutic approach fighting against these viruses. However, the role of STING in the control of RNA virus infection remains largely unexplored. In this study, using dimeric amidobenzimidazole (diABZI), a newly discovered synthetic small molecule STING receptor agonist with much higher potency than CDNs, we found that activation of STING elicits potent antiviral effects against parainfluenza virus type 3 (PIV3) and human rhinovirus 16 (HRV16), two representative respiratory viral pathogens. Notably, while anti-PIV3 activity was depend on the induction of type I interferon responses through TANK-binding kinase 1 (TBK1), anti-HRV16 activity required the induction of autophagy-related gene 5 (ATG5)-dependent autophagy, indicating that two distinct antiviral mechanisms are engaged upon STING activation. Antiviral activity and individual specific pathway was further confirmed in infected primary bronchial epithelial cells. Our findings thus demonstrate the distinct antiviral mechanisms triggered by STING agonist and uncover the potential of therapeutic effect against different viruses.

1. Introduction

Stimulator of interferon genes (STING) is a signaling molecule located in the endoplasmic reticulum (ER) and is essential for the activation of host innate immune responses against microbial infections (Barber, 2015). Upon binding of its cyclic dinucleotides (CDNs) ligand produced by the cyclic GMP-AMP synthase (cGAS) or invading bacteria, STING is activated. The activation of STING leads to the recruitment and activation of TANK-binding kinase 1 (TBK1), which phosphorylates and activates the transcription factor interferon regulatory factor 3 (IRF3) to initiate the transcription of innate immune genes with antiviral functions, such as type I interferons (IFN) and interferon stimulated genes (ISGs) (Suresh and Mosser, 2013). Recently, STING activation has been reported to induce autophagy-related gene 5 (ATG5)-dependent autophagy, which mediates the clearance of DNA and viruses in the cytosol and has a crucial role in antiviral defense (Gui et al., 2019; Liu et al., 2019).

The known natural STING agonists are nucleosides guanosine (G) and/or adenosine (A)-based CDNs and several of modified CDNs are currently being pursued as immunotherapy agents for cancers. However, CDNs are susceptible to hydrolysis by phosphodiesterases and contain negatively charged phosphate groups impeding passive diffusion through the plasma membrane, which limits their the therapeutic application only to patients with accessible solid tumors via intratumoral delivery (Yum et al., 2019). Recently, the amidobenzimidazole (ABZI) family, a new class of synthetic small molecule STING agonists with physicochemical properties completely different from those of CDNs and suitable for systemic administration, was reported (Ramanjulu et al., 2018). Dimeric ABZI (diABZI) demonstrated much higher binding affinity and cellular potency than CDNs. The reported EC_{50} of

* Corresponding author.
** Corresponding author.
*** Corresponding author.
E-mail addresses: Qingyuan.zhu@roche.com (Q. Zhu), zhipeng.yan@roche.com (Z. Yan), lu.gao@roche.com (L. Gao).

https://doi.org/10.1016/j.antiviral.2020.104933
Received 22 July 2020; Received in revised form 6 September 2020; Accepted 12 September 2020
Available online 17 September 2020

STING activation is at 130 nM, which is 400 folds more potent than cGAMP) (Ramanjulu et al., 2018). Thus, ABZI-based compounds have the potential to treat a much broader scope of indications, including cancers and infectious diseases.

Soon after the discovery of STING, it became evident that STING plays a critical role in restricting many DNA viruses, including papilloma virus, herpes simplex virus 1 (HSV1), adenovirus and vaccinia virus (Dai et al., 2014; Lam et al., 2014; Reinert et al., 2016; Sunthamala et al., 2014). In contrast to its well-documented role in innate immune responses to DNA viruses, its function in controlling RNA virus infections remains largely unexplored. Although neither synthetic RNA nor the RNA virus genome directly activates STING-related signaling pathway, an accumulating body of evidence suggests that STING is also required for optimal host protection against multiple RNA viruses, including vesicular stomatitis virus (VSV), Sendai virus (SeV), dengue virus (DENV) and influenza A virus (IAV) (Aguirre et al., 2012; Holm et al., 2016; Ishikawa and Barber, 2008; Ishikawa et al., 2009). In addition, some recent studies have reported that several RNA viruses, such as DENV, severe acute respiratory syndrome (SARS) coronavirus and influenza A virus (IAV), can antagonize STING functions (Aguirre et al., 2012; Holm et al., 2016; Sun et al., 2012). Thus, whether STING agonists could exert antiviral effects against a broader range of RNA viruses than currently accepted, as well as the nature of the mechanisms by which STING suppresses the replication of RNA viruses needs further study.

Parainfluenza virus (PIV) and Rhinovirus (HRV) are among the leading causes of respiratory infections that affect human health, and there are currently no approved antiviral treatments or vaccines for these viral infections (Bloom et al., 2009). PIV is a negative-strand RNA virus belonging to the *Paramyxoviridae,* whereas HRV is a positive-strand RNA virus belonging to the *Picornaviridae*. In this study, we aimed to evaluate whether STING agonists could inhibit PIV and HRV infections, using ABZI compounds as tools, and if so, their underlying downstream mechanisms upon STING activation against infections with selected subtypes of PIV and HRV. Our results suggest that ABZI compound-mediated STING activation elicits potent antiviral effects against PIV3 and HRV16 via two distinct antiviral mechanisms.

2. Materials and methods

2.1. Small molecules

ABZI, diABZI derivative (patent application WO2017175156) and diABZI (Ramanjulu et al., 2018) were synthesized >99% purity according to patents WO2017175156 and WO2017175147, respectively. The TBK1 inhibitor BX795, 2′,3′-cGAMP and digitonin were purchased from Sigma (SML0694, SML1229 and 300,410) and autophagy inhibitor chloroquine was purchased from Selleck Chemical (S4157).

2.2. Cell lines and antibodies

Hep2 cells (ATCC, CCL-23) were cultured in DMEM/F12 medium supplied with 10% FBS (Gibco) and 1% Penicillin/Streptomycin (Sigma). H1–HeLa cells from ATCC (ATCC, CRL-1958) were cultured in DMEM supplied with 10% FBS (Gibco) and 1% Penicillin/Streptomycin (Sigma). THP-1-Dual (thpd-nfis), THP-1-Dual KO-STING (thpd-kostg), RAW-Lucia ISG (rawl-isg), RAW-Lucia ISG-KO-STING (rawl-kostg), and HEK-Blue ISG-KO-STING (hkb-isgkostg) cells were purchased from Invivogen and cultured according to manufacturer's instruction. Anti-STING (CST, 13674s), anti-ATG5 (CST, 12994s) and anti-LC3 (CST, 3868s) antibodies were obtained from Cell Signaling Technology (CST). The anti-p-IRF3 antibody (Abcam, ab76493) and anti-actin antibody (Abcam, ab8227) were purchased from Abcam. The IFNR antibody (21385–1) was purchased from PBL.

2.3. Virus

PIV3-GFP virus (Zhang et al., 2005) was purchased from Viratree (Viratree, P323) and propagated in LLC-MK2 (ATCC, CCL-7.1) cells according to the manufacturer's protocol. Enhanced GFP was inserted between the P/C/D/V and M coding regions of PIV3 (Zhang et al., 2005). Rhinovirus 16 was obtained from ATCC (ATCC, VR-283PQ) and propagated in H1–HeLa cells (Lee et al., 2015). The viruses were stored in −80 °C until use.

2.4. HRV16 cytopathogenic effect (CPE) inhibition assay

H1–HeLa cells were seeded at 10,000 cells per well in a 96-well plate. After incubation overnight, cells were infected with HRV16 virus at a multiplicity infection (MOI) of 0.01. Immediately following the addition of virus, the indicated concentration of compound was added to the culture medium and returned to 35 °C incubator for 3 days. Following incubation, cell viability was determined using a Cell Counting Kit-8 (CCK8) kit (Dojindo, Cat.CK04) and a Envision reader (PE) according to the manufacturer's protocol.

2.5. PIV3-GFP virus inhibition assay

Hep2, H1–HeLa or PBEC were seeded at 1 × 10e4 cells per well in a Cell Carrier Ultra 96-well cell culture plate one day prior to infection. After overnight incubation, cells were infected with PIV3-GFP virus addition and treated with the indicated dose of the compound in infection medium (Opti-MEM for PIV3 or Opti-MEM with 5 μg/ml TPCK treated trypsin for MPV) and returned to a 37 °C incubator for 2 days of incubation. The number and intensity of GFP puncta were determined with an enzyme-linked immune absorbent spot (ELISpot) reader (AID ELISpot vSPOT Spectrum) and quantified with AID ELISpot reader Version 7.0 software.

2.6. Reporter assay

Human THP-1 or murine RAW264.7 cells containing an interferon regulatory factor (IRF)-inducible luciferase reporter were seeded at 2 × 10e4 cells per well in 96-well plates. After overnight incubation, cells were stimulated with the indicated compound for 24 h. Luciferase activity in the supernatant was measured using Quanti-Luc assay (Invivogen) and an Envision reader (PE) according to manufacturer's instructions.

2.7. siRNA transfection

Hep2 or H1–HeLa cells were seeded at 0.5 × 10e4 cells per well in a 96-well plate. After overnight incubation, Lipofectamine RNAi MAX (Life Technologies, 13,778,100) was used according to the manufacturer's protocol to transfect cells with indicated siRNA. Forty-eight hours after transfection, the protein level of the target of interest was determined by western blotting. Anti-viral assays were performed at 24 h post transfection. The control, STING and ATG5 stealth siRNA sets were obtained from Life Technology (Assay ID s50645 siSTING and s18159 siATG5).

2.8. Western blot analysis

To determine the expression levels of cellular proteins, cells were lysed in RIPA buffer (Life Technology) containing proteinase inhibitor cocktail (Thermo Fisher). Lysates were mixed with loading buffer (Life Technology), heated at 95 °C for 5 min, and subjected to SDS-PAGE and western blotting using preset gels and a Western blot system (Life Technology) according to the manufacturer's instructions.

2.9. Real-time PCR assay

Total RNA was isolated from cells with a RNeasy Mini Kit (Qiagen), and first-strand cDNA was generated from total RNA using random primers and a reverse transcriptase system (Invitrogen). Real-time PCR was performed on a Roche Light Cycler 480 with Taqman qPCR Master Mix Universal (ABI). The primer and probe sequences for detecting HRV16 are shown below.

Forward primer: 5′- CGCTCAGCTGTTAACCCAACA - 3'.

Reverse primer: 5′- CAGCCACGCAGGCTAGAAC - 3'.

Probe: FAM 5′- TAGAGATTCCCCTCCGGCGACGG -3′ BHQ (Sachs et al., 2011).

The sequences for detecting PIV3 are shown below.

Forward primer: 5′- TGTTGAGCCTATTTGATACATTTAATGC- 3'.

Reverse primer: 5′- ATGATAGCTCCACCAGCTGATTTT- 3'.

Probe: FAM 5′- CGTAGGCAAGAAAACATAA-3′ BHQ (Hu et al., 2005).

The cycling conditions were as described previously (Hu et al., 2005; Sachs et al., 2011). The expression values were normalized to that of hGAPDH (Applied Biosystems, 4333764F).

2.10. Quantigene assay

Hep2 or H1–HeLa cells were seeded at 0.5 × 10e4 per well in 96-well plate. The cells were treated with indicated compound for 24hr. The sample were collected from cells by Quantigene cell culture sample processing kit (Life Technology), then subjected to Quantigene multiplex kits (Life Technology) for Luminex reader according to manufacturer's instructions.

2.11. Primary bronchial epithelial cells (PBEC)

PBEC was obtained from ATCC (PCS-300-010, Lot 64,079,185). Cells were revived and cultured in ATCC epithelial cell basal medium supplied with ATCC epithelial cells growth kit (PCS-300-040). A total of 5 × 10e4 cells/ml in 0.1ml/0.5 ml of growth medium were seeded in collagen coated 96 or 24-well plate. Cells were cultured for at least 24 h and were then used for different anti-viral assays.

2.12. Statistical analysis

Statistical analysis was performed using Prism software (GraphPad). A value of $P < 0.05$ was considered statistically significant.

3. Results

3.1. The ABZI-based STING receptor agonists stimulate the IRF pathway via STING

The chemical structures of two small molecule ABZI-based STING receptor agonists are shown in Fig. 1A. The ABZI compound was derived from the original hits identified through high-throughput screening of small molecules competing with cGAMP for binding to STING. The diABZI compound with enhanced binding affinity and cellular functions is a designed dimer of the key binding element of ABZI linked through a four-carbon linker to synergize the effect of the two symmetry-related ABZI-based compounds (Ramanjulu et al., 2018). The ability of these compounds to activate the STING pathway was first evaluated using a THP-1 IRF-inducible luciferase reporter cell line, which is a human monocytic cell line containing a secreted luciferase reporter gene under the control of an IRF-inducible promoter. The natural STING ligand cGAMP activated the reporter only in wild type but not in STING knockout (KO) cells, thus validating this assay (Fig. 1B and C). We observed that both the ABZI and diABZI compounds activated the IRF reporter in a dose-dependent manner (Fig. 1B). Compared to the 2 μM half-maximal effective concentration (EC_{50}) value of ABZI, diABZI showed a much higher potency, with an EC_{50} value of 0.013 μM. In contrast, there was no induction of IRF reporter in STING KO THP-1 cells, which confirmed that the IRF pathway activation induced by the ABZI compounds is STING-dependent (Fig. 1B). Similar results were observed when a murine macrophage-derived cell line, RAW264.7, was used, suggesting that unlike the murine STING selective agonist DMXAA (Conlon et al., 2013), the ABZI-based STING receptor agonists can activate both human and murine STING with similar potency (Fig. 1C). With activities much improved over that of cGAMP (Fig. 1B and C), these non-nucleotide ABZIs represent a novel class of synthetic STING receptor agonists with the potential to be further developed for therapeutic applications.

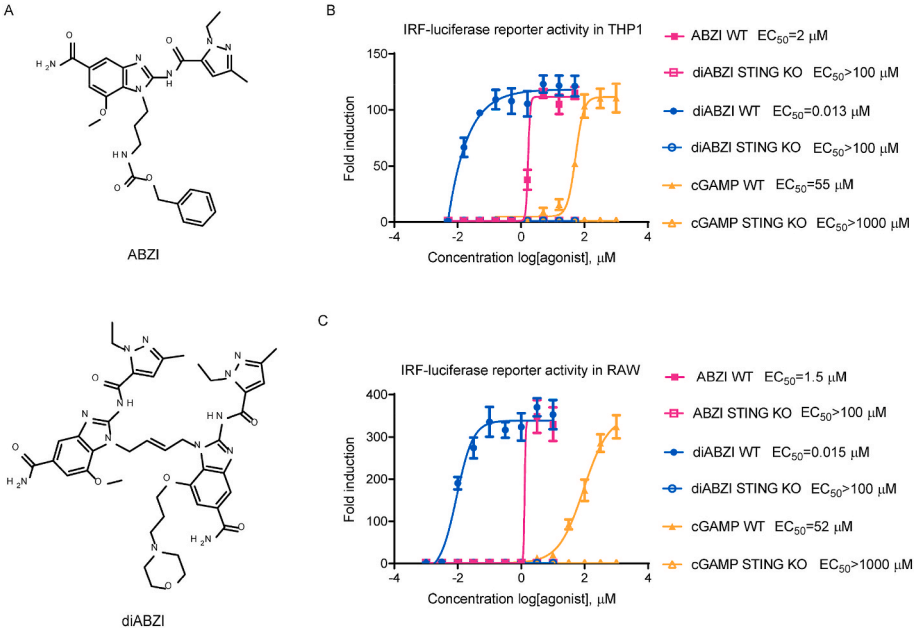

Fig. 1. STING agonist stimulates the IRF pathway via STING in both human and mouse cells. (A) The chemical structures of ABZI-based STING receptor agonists. **(B)** Wild-type or STING knockout human THP-1 or **(C)** mouse RAW264.7 IRF-inducible luciferase reporter cells were treated with indicated compounds at various concentrations for 24 h and the culture supernatants were collected for luciferase activity determination. The fold induction relative to DMSO treatment was plotted. The EC_{50} values were calculated using Prism software. The data are presented as the means ± SDs of triplicate samples from one experiment and are representative of at least three independent experiments.

3.2. The STING agonist diABZI exhibits potent anti-PIV3 and anti-HRV16 activity

Next, we sought to determine the antiviral activity of the ABZI-based STING agonists against selected subtypes of PIV and HRV. PIV3, which belongs to one of the four subtypes of PIV, is endemic year-round and can cause serious viral respiratory tract disease in infants and children (Bloom et al., 2009). HRV is the most common cold-causing virus and it can be classified into major and minor groups based on the use of cellular receptors. HRV16 belongs to the major group, which binds human intercellular adhesion molecule 1 (ICAM-1) (Greve et al., 1989). First, GFP-labelled PIV3 virus (PIV3-GFP) was used to infect Hep2 cells seeded in 96-well plates at an MOI of 0.01 in the presence of STING agonists. Two days after infection, the cells were fixed, and green fluorescence images of each well were acquired with a fluorescence ELISpot reader. The GFP signal intensity, which reflects the level of viral replication, was quantified. Both ABZI and diABZI dose-dependent inhibited the GFP signal, as demonstrated by the substantial, simultaneous reduction in both the number of GPF-positive spot puncta and the GFP signal intensity, suggesting that viral spread and replication were profoundly impaired (Fig. 2A and B). The half-maximal inhibitory concentration (IC_{50}) values of ABZI and diABZI to GFP signal intensity were calculated as 0.42 μM and 0.004 μM, respectively, which correlated well with their IRF inducing activity as shown in Fig. 1. In the meanwhile, no significant impact on cell viability was observed at up to 100 μM in Hep2 cells (supplementary Fig. 1A), therefore the selectivity index (SI) values

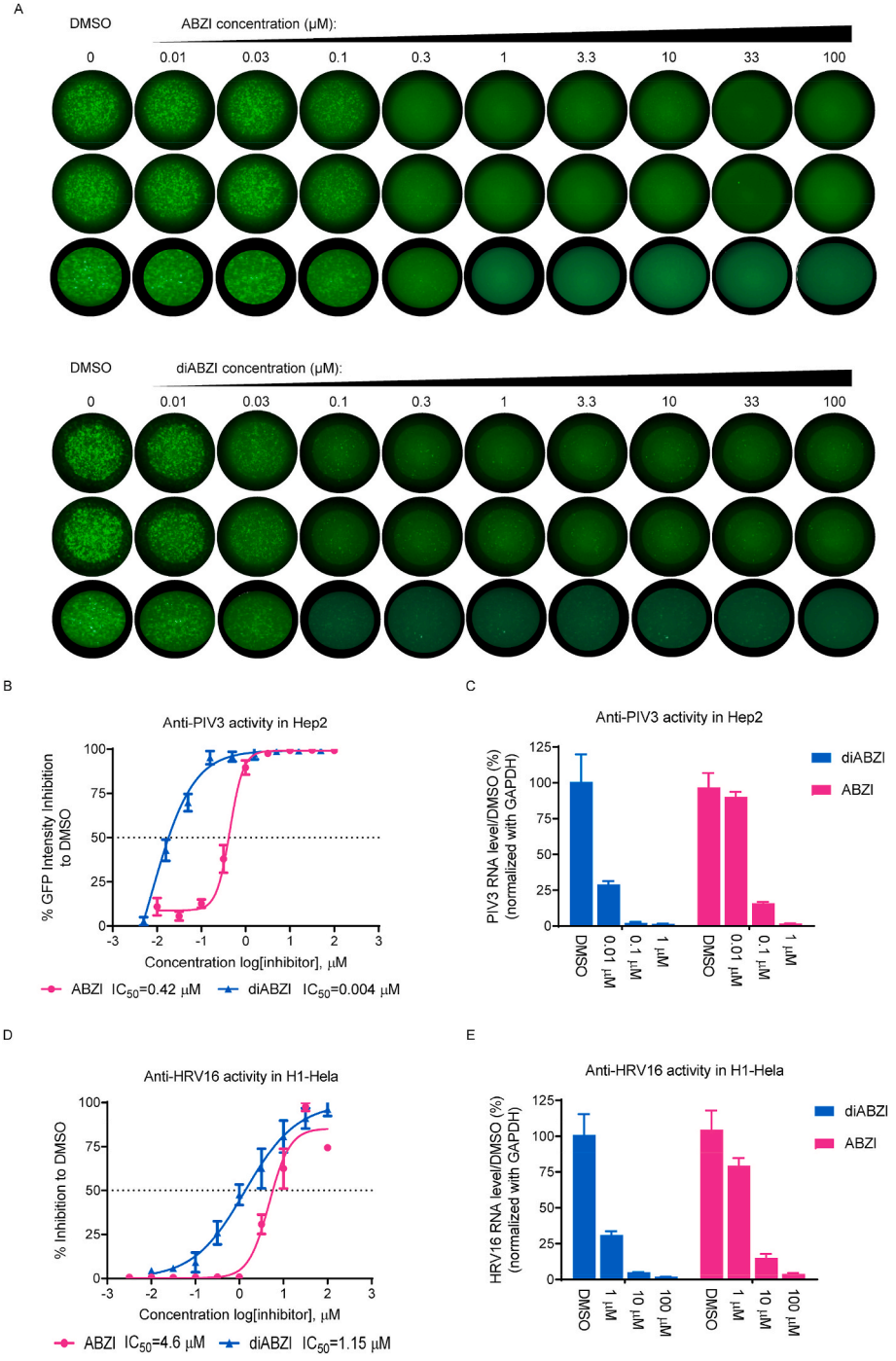

Fig. 2. STING agonist inhibits PIV and HRV replication. (A) Hep2 cells were seeded in triplicate wells of 96-well plates. The cells were infected with PIV3-GFP at MOI of 0.01 and treated with different doses of the indicated compounds for 48 h. Green fluorescence images of each well were acquired with a fluorescence ELISpot reader. **(B)** The GFP signal intensity was quantified in each well using AID ELISpot Software. The percent inhibition relative to DMSO treatment was plotted. **(C)** 24 h after PIV3-GFP infection (MOI = 0.01), total cellular RNA was isolated and reverse transcribed to cDNA. Viral RNA and GAPDH mRNA levels were then quantified via RT-PCR. The PIV3 RNA levels were normalized to the GAPDH mRNA leveland the percentage inhibition relative to DMSO treatment were plotted. **(D)** H1–HeLa cells were infected with HRV16 at MOI of 0.01 and treated with indicated concentrations of ABZI or diABZI for 72 h. The CPE was determined by a CCK-8 assay and the percent inhibition relative to DMSO treatment was plotted. **(E)** 24 h after HRV16 infection (MOI = 0.01), total cellular RNA was isolated and reverse transcribed to cDNA. Viral RNA and GAPDH mRNA levels were then quantified via RT-PCR. The HRV16 RNA levels were normalized to the GAPDH mRNA leveland the percentage inhibition relative to DMSO treatment were plotted. The IC_{50} values were calculated using Prism software. The data are presented as the means ± SDs of triplicate samples from one experiment and are representative of at least three independent experiments.

of ABZI and diABZI were calculated as >232 and > 25,000,respectively. In addition, the viral RNA levels were also measured, and the results were well correlated with the GFP intensity quantification results. (Fig. 2C).

To evaluate anti-HRV16 activity, H1–HeLa cells infected with HRV16 at an MOI of 0.01 were treated with ABZI or diABZI. After 72 h, the cell viability was measured via a CCK-8 assay to quantify cytopathic effects. Although the anti-HRV16 activity was weaker than the anti-PIV3 activity, both the ABZI and diABZI compounds dose-dependently protected the cells from CPEs, with IC_{50} values of 4.68 μM and 1.14 μM, respectively, indicating a significant anti-HRV16 activity (Fig. 2D). In addition, the half-maximal cytotoxic concentration (CC_{50}) values of both compounds were greater than 100 μM in H1–HeLa cells, suggesting that the observed antiviral effects were not related to nonspecific cytotoxicity (supplementary Fig. 1B), therefore the selectivity index (SI) values of ABZI and diABZI were calculated as >21.4 and > 87.7, respectively. In addition, the viral RNA levels were also measured and the results were correlated with the CPE assay results (Fig. 2E).

In contrast to the strong antiviral activity of the diABZI STING agonist, the natural STING ligand cGAMP, showed only modest anti-PIV3 and anti-HRV16 activity at high concentrations in the presence of digitonin permeabilization (supplementary Fig. 1C and 1D). Collectively, these results show that the diABZI STING agonist, but not cGAMP (with digitonin permeabilization), has potent anti-PIV3 and anti-HRV16 activity.

3.3. The antiviral activity of diABZI depends on STING

To determine whether the antiviral activity of the diABZI compound depends on STING, we investigated the impact of reducing STING expression on the antiviral potency of the diABZI compound. To this end, we first used siRNA to knockdown the expression of STING in Hep2 and H1–HeLa cells. Three STING targeting siRNAs were tested and siSTING-1, which demonstrated the highest knockdown efficiency in both cell lines as assessed by western blotting, was selected (Fig. 3A). siSTING-1 was transfected into Hep2 or H1–HeLa cells for 24 h, the cells were then infected with PIV3-GFP or HRV16, respectively, in the presence of diABZI. Knockdown of STING dramatically reduced the anti-PIV3 activity of diABZI in Hep2 cells and completely abolished the anti-HRV16 activity of diABZI in H1–HeLa cells (Fig. 3B and C). In addition, the anti-PIV3 and anti-HRV16 activity of diABZI were completely abolished in STING knockout HEK cells, but were fully restored via exogenous expression of STING (supplementary Fig. 2).

Moreover, similar to the results shown in Fig. 2, diABZI exhibited much stronger activity against PIV3 than against HRV16 activity (supplementary Fig. 3B and 3C). To further characterize the antiviral effect of diABZI, time-of-addition experiments were performed to determine the effects of varying the treatment initiation time of the STING agonist diABZI on the replication of PIV3 and HRV16. Hep2 cells and H1–HeLa cells were infected with PIV3-GFP and HRV16, respectively, at an MOI of 0.01, and diABZI was added at different time points during viral infection. The anti-PIV3 activity of diABZI was minimally affected even when the treatment was initiated at 24 h after infection (Fig. 3D). In contrast, delaying treatment initiation time point substantially impaired the anti-HRV16 activity of diABZI, and no antiviral effect was observed when diABZI was added at 24 h after infection (Fig. 3E).

In summary, although these results confirmed that the antiviral activity of STING agonist diABZI is dependent on STING expression, the antiviral mechanisms against PIV and HRV infections engaged upon STING activation may differ.

3.4. STING activation inhibits PIV3 and HRV16 via distinct mechanisms

Activation of STING leads to the induction of type I interferon (IFN)

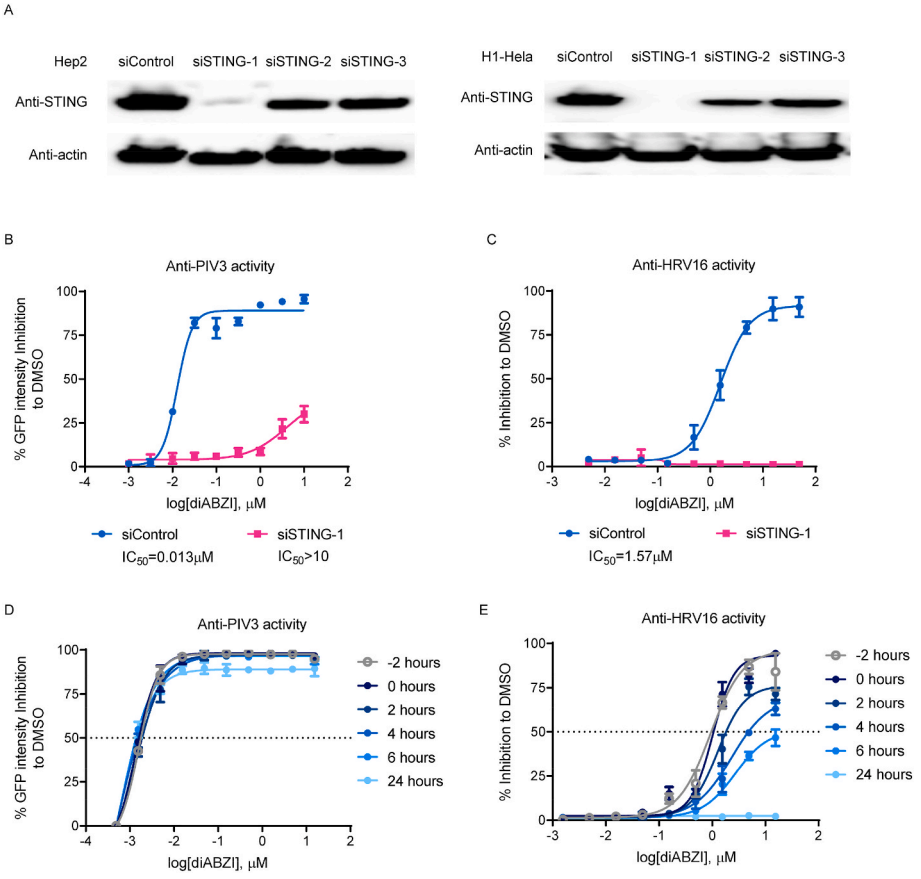

Fig. 3. The Antiviral activity of the STING receptor agonist depends on STING expression. (A) Hep2 (left panel) or H1–HeLa (right panel) cells were transfected with 20 pM STING-targeted siRNA (siSTING-1, 2, or 3) or control siRNA (siControl) and the knockdown efficiency was determined by western blotting after 48 h. **(B)** Hep2 or **(C)** H1–HeLa cells were transfected with 20 pM STING-targeted siSTING-1 for 24 h and were infected with PIV3-GFP at MOI of 0.01 (Hep2) or with HRV16 at an MOI of 0.01 (H1–HeLa) and treated with diABZI at the indicated concentrations for 48 h (Hep2) or 72 h (H1–HeLa). To determine the anti-PIV activity, the GFP signal intensity was quantified (left panel). To determine the anti-HRV activity, the CPE was assessed by a CCK-8 assay (right panel). The percent inhibition relative to DMSO treatment was plotted. **(D)** Hep2 cells were infected with PIV3-GFP at an MOI of 0.01 and treated with different doses of diABZI at the indicated times. After 48 h, the GFP signal intensity was quantified and the percent inhibition relative to DMSO treatment was plotted. **(E)** H1–HeLa cells were infected with HRV16 at an MOI of 0.01 and treated with different doses of diABZI at the indicated times. After 72 h, the CPE was determined by a CCK-8 assay and the percent inhibition relative to DMSO treatment was plotted. The data are presented as the means ± SDs of triplicate samples from one experiment and are representative of at least three independent experiments.

responses via TBK1, which are believed to play critical roles in the control of certain viral infections. In addition, recent reports demonstrate that STING also directly activates autophagy, which is important for the clearance of DNA and viruses in the cytosol (Gui et al., 2019; Liu et al., 2019). Consistent with previous reports, in Hep2 and H1–HeLa cells treated with diABZI, we observed clear activation of both the IRF and autophagy pathways, as indicated by the increased levels of phosphorylated-IRF3 (p-IRF3) and LC3-II conversion (Fig. 4A). Therefore, to determine the contribution of these two pathways to the antiviral activity of diABZI, the TBK1 inhibitor BX795 or the autophagy inhibitor chloroquine (CQ) was applied during diABZI treatment. In both PIV3-infected Hep2 and H1–HeLa cells, BX795 completely abolished the anti-PIV3 activity of diABZI, whereas no significant impairment was observed with CQ treatment, suggesting that the activation of immune responses via TBK1 plays a dominant role in STING-mediated anti-PIV3 activity (Fig. 4B and C). Interestingly, CQ, but not BX795, substantially reduced the anti-HRV16 activity of diABZI, suggesting that the induction of the autophagy pathway plays a major role in STING-mediated anti-HRV16 activity, in sharp contrast to the effect seen on STING-mediated anti-PIV3 activity (Fig. 4D). In addition, neither CQ nor BX795 at test concentration do not affected the GFP intensity of PIV3, as well as the CPE ability of HRV16 at test concentration (supplementary Fig. 3).

Consistent with these observations, we found that Pegasys (Pegylated interferon 2alpha) treatment greatly suppressed the replication of PIV3, but not HRV16 (supplementary Fig. 4A and 4B). Furthermore, blocking the type I interferon receptor (IFNR) with a neutralizing antibody modestly affected the anti-PIV3 activity of diABZI, but did not affect its anti-HRV16 activity (supplementary Fig. 4C, 4D and 4E). In addition, we observed similar inductions in the expression of several

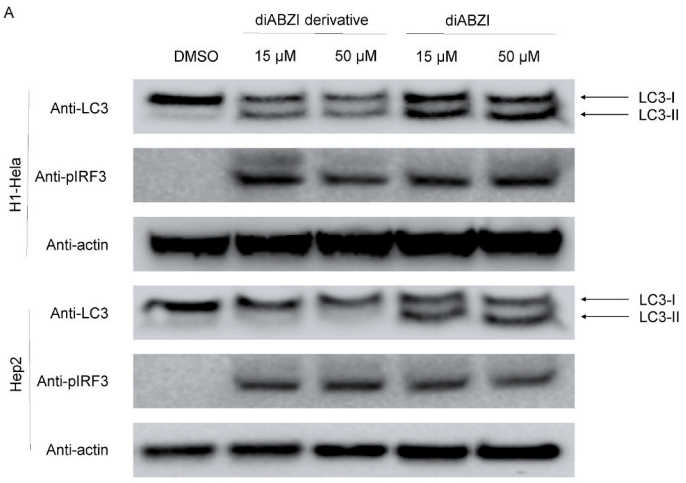

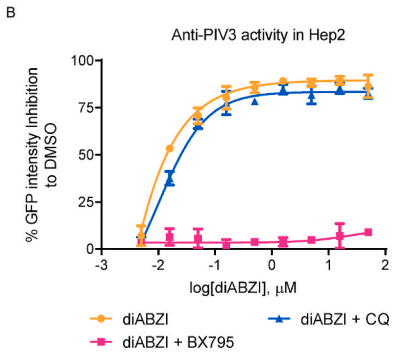

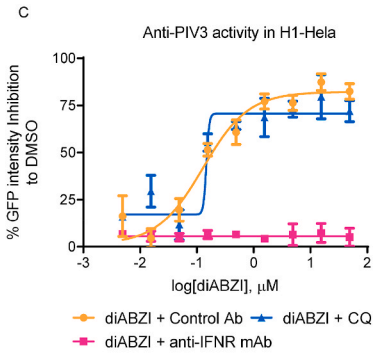

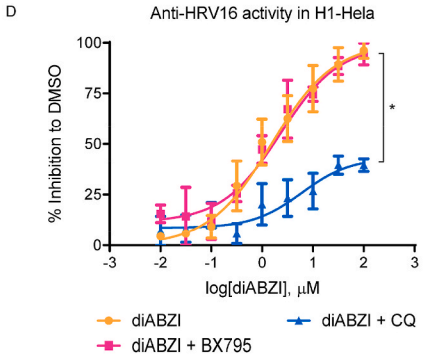

Fig. 4. The STING receptor agonist inhibits PIV and HRV through distinct mechanisms. (A) H1–HeLa (upper panels) or Hep2 (lower panels) cells were treated with the indicated concentrations of diABZI or diABZI derivative for 24 h. Cells were lysed and lysates were subjected to Western blot analysis of LC3, p-IRF3 and actin with specific antibodies. **(B)** Hep2 or **(C)** H1–HeLa cells were infected with PIV3-GFP at an MOI of 0.01 and treated with the indicated concentrations of diABZI in the presence or absence of 1 μM (Hep2)/5 μM (H1–HeLa) of TBK1 inhibitor (TBKi, BX795) or 50 μM (Hep2)/25 μM (H1–HeLa) CQ for 48 h. The GFP signal intensity was quantified and the percent inhibition relative to DMSO treatment was plotted. **(D)** H1–HeLa cells were infected with HRV16 at an MOI of 0.01 and treated with the indicated concentrations of diABZI in the presence or absence of 5 μM TBKi (BX795) or 25 μM CQ for 72 h. The CPE was determined by a CCK-8 assay and the percent inhibition relative to DMSO treatment was plotted. The data are presented as the means ± SDs of triplicate samples from one experiment and are representative of at least three independent experiments. $^{*}P < 0.05$, $^{**}P < 0.01$.

representative ISG mRNAs upon diABZI treatment in the presence or absence of viral infection, indicating that the STING downstream signaling pathway is not affected by viral infection (supplementary Fig. 5). These results support the hypothesis that IFN responses significantly contribute to the anti-PIV3 activity, but not the anti-HRV16 activity of diABZI, mediated by STING activation. Furthermore, knockdown ATG5 expression, which is required for STING-induced autophagy, completely abolished anti-HRV16, but not anti-PIV3 activity of diABZI (supplementary Fig. 6).

Interestingly, we found a diABZI derivative could induce p-IRF3 in both Hep2 and H1-Hela cell, but with a much weaker ability to induce LC3-II conversion (supplementary Fig. 7A and Fig. 4A). Moreover, this compound demonstrated strong anti-PIV3 activity ($IC_{50} = 0.1$ μM), but without any anti-HRV16 activity ($IC_{50} > 100$ μM, supplementary 7B). Further studies are warranted to better understand the mechanistic differences engaged by the diABZI and diABZI derivative compounds.

Taken together, these results suggest that STING activation inhibits PIV3 and HRV16 via activation of the TBK1-mediated IFN responses and induction of autophagy, respectively.

3.5. Antiviral activity of STING agonist diABZI in human primary bronchial epithelial cells (PBECs)

Immortalized cell lines, such as Hep2 and HeLa, which can be conveniently cultured to support robust viral replication, have been used extensively to study virus–host interactions. However, these cell lines are poorly representative of the complexity of the respiratory epithelium. PBECs are the primary targets of many respiratory viruses *in vivo*, including PIV and HRV, and are thus a more physiologically relevant model for studying these viruses (Bossios et al., 2005; Moskwa et al., 2018). Therefore, we sought to determine whether the STING agonist diABZI could inhibit PIV and HRV replication in PBECs. To this end, PBECs were seeded in collagen-coated plates and were then infected with PIV3-GFP or HRV16 in the presence of diABZI. For PIV3-GFP-infected cells, at 48 h after infection, green fluorescence images of each wells were acquired with a fluorescence ELISpot reader. The GFP signal intensity was quantified, and the inhibition percentage relative to DMSO treatment was plotted (Fig. 5A and B). The IC_{50} value was calculated as 0.01 μM, which was similar to that observed in Hep2

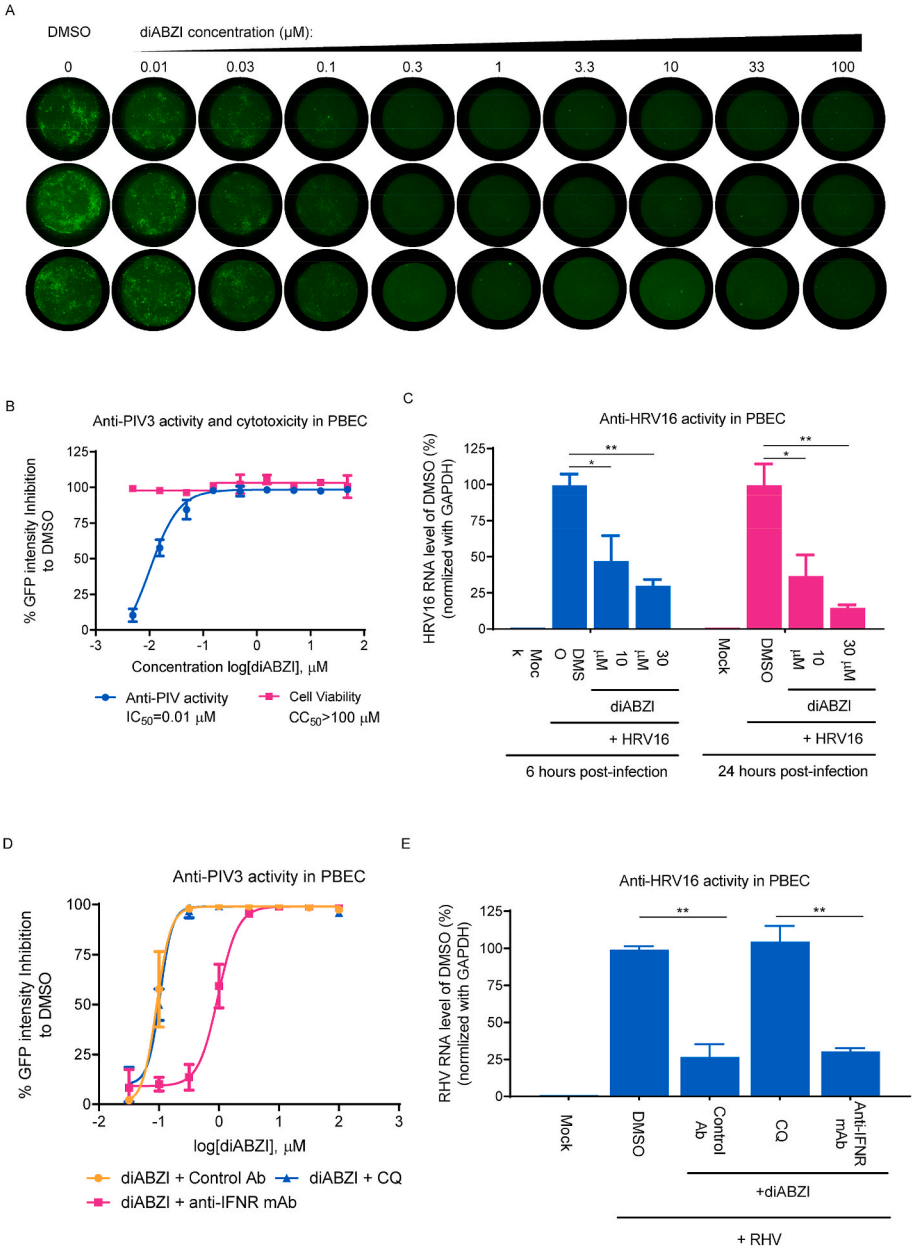

Fig. 5. The STING agonist exhibits anti-PIV3 and anti-HRV16 activity in PBECs. **(A)** PBECs were seeded in triplicate wells of collagen-coated 96-well plates, infected with PIV3-GFP at an MOI 0.001 and treated with the indicated concentrations of diABZI for 48 h. Green fluorescence images of each well were acquired with a fluorescence ELISpot reader. **(B)** The GFP signal intensity was quantified and the percent inhibition relative to DMSO treatment was plotted. The IC_{50} values were calculated using Prism software. **(C)** PBECs were infected with HRV16 at an MOI of 10 and treated with the indicated concentrations of diABZI for 6 h or 24 h. Total cellular RNA was isolated and reverse transcribed to cDNA. Viral RNA and GAPDH mRNA were then quantified via RT-PCR. The HRV RNA level was normalized to the GAPDH mRNA level and the percent inhibition relative to DMSO treatment was plotted. **(D)** PBECs were seeded on collagen-coated 96-well plates, then infected with PIV3-GFP at an MOI 0.001 and treated with the indicated concentrations of diABZI in the presence or absence of CQ (50 μM)/IFNR antibody (anti-IFNR mAb 5 μg/ml)/isotype control antibody (control mAb, 5 μg/ml) for 48 h. The GFP signal intensity was quantified and the percent inhibition relative to DMSO treatment was plotted. **(E)** PBECs were infected with HRV16 at an MOI of 10 and treated with 30 μM of diABZI for 24 h in the presence or absence of CQ (50 μM)/IFNR antibody (anti-IFNR mAb 5 μg/ml)/isotype control antibody (control mAb, 5 μg/ml). Total cellular RNA was isolated and reverse transcribed to cDNA. Viral RNA and GAPDH mRNA were then quantified via RT-PCR. The HRV RNA level was normalized to the GAPDH mRNA level and the percent inhibition relative to DMSO treatment was plotted. The data are presented as the means ± SD of triplicate samples from one experiment and are representative of at least three independent experiments. $^{*}P < 0.05$, $^{**}P < 0.01$.

cells.

HRV16 infection did not cause apparent CPEs in PBECs (data not shown). Therefore, we harvested the cells and measured the viral RNA level with RT-PCR at 6 h and 24 h after infection. We observed a substantial reduction in the HRV16 RNA level upon diABZI treatment, confirming its anti-HRV16 activity (Fig. 5C).

In addition, the pathway analysis experiments were also conducted in PBECs. We observed that CQ, but not anti-IFNR antibody, blocked HRV16 replication, while anti-IFNR mAb, but not CQ, inhibited PIV3 replication in PBECs, which were consistent with the results from cell lines (Fig. 5D and E). In summary, using virus-infected PBECs, we further confirmed the antiviral activity and distinct antiviral mechanisms induced by STING activation.

4. Discussion

The host innate immune system acts as the first line of defense against viral infections. As an essential innate signaling molecule, STING is required for protecting the host against a broad range of viral infections. Thus, STING agonists has the potential to be developed as broad-spectrum antiviral agents. However, CDNs type agonists derived from natural STING ligands have stability and permeability issues that limit their therapeutic applications. Using the newly discovered diABZI STING agonist as a tool, we demonstrated potent antiviral activity against the representative respiratory RNA viruses, PIV3 and HRV16, upon STING activation. Compared to cGAMP, diABZI showed a much stronger ability to trigger STING activation, which correlated well with its high antiviral potency. We speculate that this enhanced cellular performance is likely derived from its improved permeability (data not shown). In addition to the highly differentiated physicochemical properties and increased STING binding affinity of ABZI-based agonists compared with CDNs, these agonists efficiently activate STING in an open conformation without the need for lid closure, which may also contribute to their improved potency (Ramanjulu et al., 2018).

Similar to many other RNA viruses, such as HCV, VSV and SeV, PIV3 is highly sensitive to IFN treatment (Rabbani et al., 2016). Type I IFN treatment has been reported to efficiently block PIV3 replication by inducing the expression of ISGs with antiviral functions (Atreya and Kulkarni, 1999; Rabbani et al., 2016). It has been well-characterized that STING activation leads to type I IFN production and ISGs induction (Ishikawa and Barber, 2008). Indeed, diABZI strongly suppressed PIV3 replication with a similar potency across all cell culture systems tested, which correlated well with its IRF induction activity. However, some RNA viruses, such as respiratory syncytial virus (RSV), which belongs to the same *Paramyxoviridae* as PIV, as well as HRV16, are resistant to IFN treatment (supplementary Fig. 3E) (Atreya and Kulkarni, 1999). Consistent with these results, we observed much reduced potency against HRV16 and RSV upon diABZI treatment, implying the resistance of these viruses to the conventional IFN response-driven antiviral mechanisms (Fig. 2C and data not shown). It is unlikely that the virus actively antagonizes IFN responses, as we did not observe a significant difference in the ISG mRNA levels between infected and non-infected cells upon diABZI treatment (supplementary Fig. 4).

Despite its resistance to host IFN responses, diABZI showed clear dose-dependent anti-HRV16 activity, with an IC_{50} in the micro molar range, which was not affected by treatment with the TBK1 inhibitor BX795 or the IFNR blocking antibody, indicating that other antiviral mechanisms might be involved (Figs. 4D and 5C). Indeed, using CQ and siRNA knockdown, we confirmed that ATG5-dependent autophagy triggered by STING activation is responsible for the anti-HRV16 activity of diABZI (Fig. 4D and supplementary Fig. 5C).

Autophagy is a major pathway for degradation of cellular components inside eukaryotic cells (Fader and Colombo, 2009). Viruses have coevolved strategies to manipulate this pathway to ensure their own replication and advantage. Most previous studies focused on the proviral mechanisms of autophagy in infected cells. However, PIV and HRV have been reported to induce and subvert the autophagic machinery to promote their own replication (Ding et al., 2014; Klein and Jackson, 2011). Interleukin-1 receptor-associated kinase M (IRAK-M) promotes human rhinovirus infection of lung epithelial cells via the autophagic pathway (Wu et al., 2013). However, accumulating evidence suggests that autophagy also contributes to the host defense against microbial infections (Rey-Jurado et al., 2015). Induction of autophagy has been shown to inhibit the growth of VSV and HSV1 (Orvedahl et al., 2007; Shelly et al., 2009). Furthermore, STING induced autophagy restricts ZIKV infection in the adult fly brain (Liu et al., 2018). Picornaviruses, such as poliovirus (PV) and HRV, permeabilize endosomes to deliver their genomes into the cytoplasm, where they can be detected and inhibited by galectin-8 via autophagic degradation (Staring et al., 2017). In addition, the results of the time-of-addition experiments result suggest that diABZI functions early during HRV16 infection and that delaying treatment initiation substantially impacts its antiviral efficacy. Therefore, the anti-HRV16 activity observed upon STING activation is likely driven by autophagy-mediated virion degradation, thus viral genome release is prevented.

Interestingly, diABZI showed much lower potency against HRV16 than against PIV3, and this discrepancy cannot be explained by assay methodologies and endpoint differences. The autophagy-mediated antiviral response, which targets only early steps in the viral life cycle, is likely less efficient than the IRF-mediated antiviral response which is believed to block multiple steps in the viral life cycle via induction of IFN and ISGs. Alternatively, induction of the autophagy-mediated antiviral response may have slower kinetics or require a higher STING agonist concentration than induction of the IFN response. Further studies are thus needed to elucidate the details regarding the difference in the potency of diABZI against different type of viruses.

In this study, the diABZI STING agonist demonstrated potent antiviral activity against multiple respiratory RNA viruses, represented by PIV3 and HRV16, which broadly affect human health and have no effective treatment or vaccine. Therefore, STING agonists hold promise further development as therapeutic or prophylactic agents in respiratory infections caused by these viruses. However, caution is required, because STING activation also induces the production of pro-inflammatory cytokines, such as IL-1β, IL-6, and TNF-α, which may exacerbate inflammation-related symptoms (Chen et al., 2016). Thus, the timing, dose level and duration of the treatment with STING agonists need to be evaluated carefully to prevent exacerbated inflammation. Further *in vivo* studies are imperative to better understand the therapeutic efficacy and safety of STING agonist against respiratory virus infections.

Author contribution

Q.Z., Z.Y. and L.G. designed research; Q.Z.and H.H. performed research; H.L. and H.S. contributed new reagents; Q.Z, Z.Y and L.G. analyzed data; and Q.Z., Z.Y. and L.G. wrote the paper.

Funding

This work was supported by F. Hoffman-La Roche Ltd.

Declaration of competing interest

The authors are employees of F. Hoffman-La Roche Ltd.

Appendix A. Supplementary data

Supplementary data to this article can be found online at https://doi.org/10.1016/j.antiviral.2020.104933.

References

Aguirre, S., Maestre, A.M., Pagni, S., Patel, J.R., Savage, T., Gutman, D., Maringer, K., Bernal-Rubio, D., Shabman, R.S., Simon, V., Rodriguez-Madoz, J.R., Mulder, L.C., Barber, G.N., Fernandez-Sesma, A., 2012. DENV inhibits type I IFN production in infected cells by cleaving human STING. PLoS Pathog. 8, e1002934.

Atreya, P.L., Kulkarni, S., 1999. Respiratory syncytial virus strain A2 is resistant to the antiviral effects of type I interferons and human MxA. Virology 261, 227–241.

Barber, G.N., 2015. STING: infection, inflammation and cancer. Nat. Rev. Immunol. 15, 760–770.

Bloom, B., Cohen, R.A., Freeman, G., 2009. Summary health statistics for U.S. Children: national health interview survey, 2008. Vital Health Stat 10, 1–81.

Bossios, A., Psarras, S., Gourgiotis, D., Skevaki, C.L., Constantopoulos, A.G., Saxoni-Papageorgiou, P., Papadopoulos, N.G., 2005. Rhinovirus infection induces cytotoxicity and delays wound healing in bronchial epithelial cells. Respir. Res. 6, 114.

Chen, Q., Sun, L., Chen, Z.J., 2016. Regulation and function of the cGAS-STING pathway of cytosolic DNA sensing. Nat. Immunol. 17, 1142–1149.

Conlon, J., Burdette, D.L., Sharma, S., Bhat, N., Thompson, M., Jiang, Z., Rathinam, V.A., Monks, B., Jin, T., Xiao, T.S., Vogel, S.N., Vance, R.E., Fitzgerald, K.A., 2013. Mouse, but not human STING, binds and signals in response to the vascular disrupting agent 5,6-dimethylxanthenone-4-acetic acid. J. Immunol. 190, 5216–5225.

Dai, P., Wang, W., Cao, H., Avogadri, F., Dai, L., Drexler, I., Joyce, J.A., Li, X.D., Chen, Z., Merghoub, T., Shuman, S., Deng, L., 2014. Modified vaccinia virus Ankara triggers type I IFN production in murine conventional dendritic cells via a cGAS/STING-mediated cytosolic DNA-sensing pathway. PLoS Pathog. 10, e1003989.

Ding, B., Zhang, G., Yang, X., Zhang, S., Chen, L., Yan, Q., Xu, M., Banerjee, A.K., Chen, M., 2014. Phosphoprotein of human parainfluenza virus type 3 blocks autophagosome-lysosome fusion to increase virus production. Cell Host Microbe 15, 564–577.

Fader, C.M., Colombo, M.I., 2009. Autophagy and multivesicular bodies: two closely related partners. Cell Death Differ. 16, 70–78.

Greve, J.M., Davis, G., Meyer, A.M., Forte, C.P., Yost, S.C., Marior, C.W., Kamarck, M.E., Mcclelland, A., 1989. The major human rhinovirus receptor is icam-1. Cell 56, 839–847.

Gui, X., Yang, H., Li, T., Tan, X., Shi, P., Li, M., Du, F., Chen, Z.J., 2019. Autophagy induction via STING trafficking is a primordial function of the cGAS pathway. Nature 567, 262–266.

Holm, C.K., Rahbek, S.H., Gad, H.H., Bak, R.O., Jakobsen, M.R., Jiang, Z., Hansen, A.L., Jensen, S.K., Sun, C., Thomsen, M.K., Laustsen, A., Nielsen, C.G., Severinsen, K., Xiong, Y., Burdette, D.L., Hornung, V., Lebbink, R.J., Duch, M., Fitzgerald, K.A., Bahrami, S., Mikkelsen, J.G., Hartmann, R., Paludan, S.R., 2016. Influenza A virus targets a cGAS-independent STING pathway that controls enveloped RNA viruses. Nat. Commun. 7, 10680.

Hu, A.Z., Colella, M., Zhao, P., Li, F.L., Tam, J.S., Rappaport, R., Cheng, S.M., 2005. Development of a real-time RT-PCR assay for detection and quantitation of parainfluenza virus 3. J. Virol Methods 130, 145–148.

Ishikawa, H., Barber, G.N., 2008. STING is an endoplasmic reticulum adaptor that facilitates innate immune signalling (vol 455, pg 674, 2008). Nature 456, 274-274.

Ishikawa, H., Ma, Z., Barber, G.N., 2009. STING regulates intracellular DNA-mediated, type I interferon-dependent innate immunity. Nature 461, 788–792.

Klein, K.A., Jackson, W.T., 2011. Human rhinovirus 2 induces the autophagic pathway and replicates more efficiently in autophagic cells. J. Virol. 85, 9651–9654.

Lam, E., Stein, S., Falck-Pedersen, E., 2014. Adenovirus detection by the cGAS/STING/TBK1 DNA sensing cascade. J. Virol. 88, 974–981.

Lee, W.M., Chen, Y., Wang, W., Mosser, A., 2015. Growth of human rhinovirus in H1-HeLa cell suspension culture and purification of virions. Methods Mol. Biol. 1221, 49–61.

Liu, Y., Gordesky-Gold, B., Leney-Greene, M., Weinbren, N.L., Tudor, M., Cherry, S., 2018. Inflammation-induced, STING-dependent autophagy restricts zika virus infection in the Drosophila brain. Cell Host Microbe 24, 57–68 e53.

Liu, D., Wu, H., Wang, C., Li, Y., Tian, H., Siraj, S., Sehgal, S.A., Wang, X., Wang, J., Shang, Y., Jiang, Z., Liu, L., Chen, Q., 2019. STING directly activates autophagy to tune the innate immune response. Cell Death Differ. 26 (9), 1735–1749. https://doi.org/10.1038/s41418-018-0251-z.

Moskwa, S., Piotrowski, W., Marczak, J., Pawelczyk, M., Lewandowska-Polak, A., Jarzebska, M., Brauncajs, M., Globinska, A., Gorski, P., Papadopoulos, N.G., Edwards, M.R., Johnston, S.L., Kowalski, M.L., 2018. Innate immune response to viral infections in primary bronchial epithelial cells is modified by the atopic status of asthmatic patients. Allergy Asthma Immunol Res 10, 144–154.

Orvedahl, A., Alexander, D., Talloczy, Z., Sun, Q., Wei, Y., Zhang, W., Burns, D., Leib, D. A., Levine, B., 2007. HSV-1 ICP34.5 confers neurovirulence by targeting the Beclin 1 autophagy protein. Cell Host Microbe 1, 23–35.

Rabbani, M.A., Ribaudo, M., Guo, J.T., Barik, S., 2016. Identification of interferon-stimulated gene proteins that inhibit human parainfluenza virus type 3. J. Virol. 90, 11145–11156.

Ramanjulu, J.M., Pesiridis, G.S., Yang, J., Concha, N., Singhaus, R., Zhang, S.Y., Tran, J. L., Moore, P., Lehmann, S., Eberl, H.C., Muelbaier, M., Schneck, J.L., Clemens, J., Adam, M., Mehlmann, J., Romano, J., Morales, A., Kang, J., Leister, L., Graybill, T.L., Charnley, A.K., Ye, G., Nevins, N., Behnia, K., Wolf, A.I., Kasparcova, V., Nurse, K., Wang, L., Puhl, A.C., Li, Y., Klein, M., Hopson, C.B., Guss, J., Bantscheff, M., Bergamini, G., Reilly, M.A., Lian, Y., Duffy, K.J., Adams, J., Foley, K.P., Gough, P.J., Marquis, R.W., Smothers, J., Hoos, A., Bertin, J., 2018. Design of amidobenzimidazole STING receptor agonists with systemic activity. Nature 564, 439–443.

Reinert, L.S., Lopusna, K., Winther, H., Sun, C., Thomsen, M.K., Nandakumar, R., Mogensen, T.H., Meyer, M., Vaegter, C., Nyengaard, J.R., Fitzgerald, K.A., Paludan, S.R., 2016. Sensing of HSV-1 by the cGAS-STING pathway in microglia orchestrates antiviral defence in the CNS. Nat. Commun. 7, 13348.

Rey-Jurado, E., Riedel, C.A., Gonzalez, P.A., Bueno, S.M., Kalergis, A.M., 2015. Contribution of autophagy to antiviral immunity. FEBS Lett. 589, 3461–3470.

Sachs, L.A., Schnurr, D., Yagi, S., Lachowicz-Scroggins, M.E., Widdicombe, J.H., 2011. Quantitative real-time PCR for rhinovirus, and its use in determining the relationship between TCID50 and the number of viral particles. J. Virol Methods 171, 212–218.

Shelly, S., Lukinova, N., Bambina, S., Berman, A., Cherry, S., 2009. Autophagy is an essential component of Drosophila immunity against vesicular stomatitis virus. Immunity 30, 588–598.

Staring, J., von Castelmur, E., Blomen, V.A., van den Hengel, L.G., Brockmann, M., Baggen, J., Thibaut, H.J., Nieuwenhuis, J., Janssen, H., van Kuppeveld, F.J.M., Perrakis, A., Carette, J.E., Brummelkamp, T.R., 2017. PLA2G16 represents a switch between entry and clearance of Picornaviridae. Nature 541, 412.

Sun, L., Xing, Y., Chen, X., Zheng, Y., Yang, Y., Nichols, D.B., Clementz, M.A., Banach, B. S., Li, K., Baker, S.C., Chen, Z., 2012. Coronavirus papain-like proteases negatively regulate antiviral innate immune response through disruption of STING-mediated signaling. PloS One 7, e30802.

Sunthamala, N., Thierry, F., Teissier, S., Pientong, C., Kongyingyoes, B., Tangsiriwatthana, T., Sangkomkamhang, U., Ekalaksananan, T., 2014. E2 proteins of high risk human papillomaviruses down-modulate STING and IFN-kappa transcription in keratinocytes. PloS One 9, e91473.

Suresh, R., Mosser, D.M., 2013. Pattern recognition receptors in innate immunity, host defense, and immunopathology. Adv. Physiol. Educ. 37, 284–291.

Wu, Q., van Dyk, L.F., Jiang, D., Dakhama, A., Li, L., White, S.R., Gross, A., Chu, H.W., 2013. Interleukin-1 receptor-associated kinase M (IRAK-M) promotes human rhinovirus infection in lung epithelial cells via the autophagic pathway. Virology 446, 199–206.

Yum, S., Li, M., Frankel, A.E., Chen, Z.J., 2019. Roles of the cGAS-STING pathway in cancer immunosurveillance and immunotherapy. Annu. Rev. Cell Biol. 3, 323–344.

Zhang, L., Bukreyev, A., Thompson, C.I., Watson, B., Peeples, M.E., Collins, P.L., Pickles, R.J., 2005. Infection of ciliated cells by human parainfluenza virus type 3 in an in vitro model of human airway epithelium. J. Virol. 79, 1113–1124.